

See discussions, stats, and author profiles for this publication at: <https://www.researchgate.net/publication/13501111>

# Establishing a Limit of Recognition for a Vapor Sensor Array

ARTICLE *in* ANALYTICAL CHEMISTRY · NOVEMBER 1998

Impact Factor: 5.64 · DOI: 10.1021/ac980344w · Source: PubMed

---

CITATIONS

51

---

READS

32

4 AUTHORS, INCLUDING:



William A Groves

Pennsylvania State University

34 PUBLICATIONS 603 CITATIONS

SEE PROFILE

# Establishing a Limit of Recognition for a Vapor Sensor Array

Edward T. Zellers,<sup>\*,†,‡</sup> Jeongim Park,<sup>†</sup> Teresa Hsu,<sup>‡</sup> and William A. Groves<sup>§</sup>

Department of Environmental and Industrial Health and Department of Chemistry, University of Michigan, Ann Arbor, Michigan 48109-2029, and Department of Preventive Medicine and Environmental Health, University of Iowa, Iowa City, Iowa 52242-5000

**Organic vapor analysis with microsensor arrays relies principally on two output parameters: the response pattern, which provides qualitative information, and the response sensitivity, which determines the limit of detection (LOD). The latter is used to define the operating limit in the low-concentration range, under the implicit assumption that, if a vapor can be detected, it can be identified and differentiated from other vapors on the basis of its response pattern. In this study, the performance of an array of four polymer-coated surface acoustic wave vapor sensors was explored using calibrated response data from 16 solvent vapors in Monte Carlo simulations coupled with pattern recognition analysis. The statistical modeling revealed that the ability to recognize a vapor from its response pattern decreases with decreasing vapor concentration, as expected, but also that the concentration at which errors in vapor recognition become excessive is well above the calculated LOD in most cases, despite the LOD being based on the least sensitive sensor in the array. These results suggest the adoption of a limit of recognition (LOR), defined as the concentration below which a vapor can no longer be reliably recognized from its response pattern, as an additional criterion for evaluating the performance of multisensor arrays. A generalized method for estimating the LOR is presented, as well as a means for improving the LOR via residual error analysis.**

Use of a set of partially selective chemical sensors coupled with statistical pattern recognition methods provides a versatile approach to chemical analysis. Measurement of a wide range of gaseous and dissolved chemical species has been reported with this approach, using arrays of amperometric sensors,<sup>1</sup> chemiresistors,<sup>2–4</sup> optical fibers,<sup>5,6</sup> metal oxide semiconductors,<sup>7–9</sup> thickness

shear mode resonators,<sup>10–12</sup> and surface acoustic wave (SAW) sensors.<sup>13–18</sup>

For the analysis of organic solvent vapors, SAW sensors coated with rubbery amorphous polymers have proven particularly useful: responses vary in direct proportion to the extent of vapor sorption, which is typically rapid, reversible, and a linear function of vapor concentration. Since sorption depends on the strength of the nonbonding vapor–polymer interactions, an array consisting of SAW sensors coated with different functionalized polymers can provide a set of responses whose pattern can be used to identify and differentiate multiple individual vapors as well as the components of multivapor mixtures.<sup>13,16</sup>

In designing a SAW sensor array for broad-spectrum analysis of organic vapors, the goal is to select polymer coatings that provide the best tradeoff between maximizing the number of detectable vapors and maximizing the singularity of the response pattern for each vapor. This process can be facilitated by the application of physicochemical models of polymer sorption such as those originally developed for describing vapor retention behavior in gas chromatography.<sup>19–22</sup> Models based on solvation

<sup>†</sup> Department of Environmental and Industrial Health, University of Michigan.

<sup>‡</sup> Department of Chemistry, University of Michigan.

<sup>§</sup> University of Iowa.

- (1) Stetter, J.; Jurs, P. C.; Rose, S. L. *Anal. Chem.* **1986**, *58*, 860–866.
- (2) Barger, W. R.; Wohltjen, H.; Snow, A. W.; Lint, J.; Jarvis, N. L. In *Fundamentals and Applications of Chemical Sensors*; Schuetzle, D., Hammerle, R., Eds.; ACS Symposium Series 309; American Chemical Society: Washington, DC, 1986; pp 155–165.
- (3) Hatfield, J.; Neaves, P.; Hicks, P.; Persaud, K.; Travers, P. *Sens. Actuators B* **1994**, *18*, 221–228.
- (4) Grate, J. W.; Klusty, M.; Barger, W. R.; Snow, A. W. *Anal. Chem.* **1990**, *62*, 1927–1934.

- (5) White, J.; Kauer, J. S.; Dickinson, T. A.; Walt, D. R. *Anal. Chem.* **1996**, *68*, 2191–2202.
- (6) Sutter, J. M.; Jurs, P. C. *Anal. Chem.* **1997**, *69*, 856–862.
- (7) Kohl, D. In *Handbook of Biosensors and Electronic Noses*; Kress-Rogers, E., Ed.; CRC Press: Boca Raton, FL, 1997; pp 534–561.
- (8) Sundgren, H.; Vollmer, H.; Lundstrom, I. *Sens. Actuators B* **1992**, *9*, 127–131.
- (9) Gardner, J. W. *Sens. Actuators B* **1991**, *4*, 109–118.
- (10) Carey, W. P.; Kowalski, B. R. *Anal. Chem.* **1986**, *58*, 3077–3084.
- (11) Schweizer-Berberich, M.; Goppert, J.; Hierlemann, A.; Mitrovics, J.; Weimar, U.; Rosenstiel, W.; Gopel, W. *Sens. Actuators B* **1995**, *26–27*, 232–236.
- (12) Schierbaum, K. D.; Hierlemann, A.; Gopel, W. *Sens. Actuators B* **1994**, *18–19*, 448–452.
- (13) Rose-Pehrson, S. L.; Grate, J. W.; Ballantine, D. S.; Jurs, P. *Anal. Chem.* **1988**, *60*, 2801.
- (14) Wohltjen, H.; Ballantine, D. S., Jr.; Jarvis, N. L. In *Microsensors and Microinstrumentation*; ACS Symposium Series 403; Murray, R. W., Dessy, R. E., Heineman, W. R., Janata, J., Seitz, W. R., Eds.; American Chemical Society: Washington, DC, 1989; pp 157–175.
- (15) Patrash, S. J.; Zellers, E. T. *Anal. Chim. Acta* **1994**, *288*, 167.
- (16) Zellers, E. T.; Batterman, S. A.; Han, M.; Patrash, S. J. *Anal. Chem.* **1995**, *67*, 1092–1106.
- (17) Hierlemann, A.; Weimar, U.; Kraus, G.; Schweizer-Berberich, M.; Gopel, W. *Sens. Actuators B* **1995**, *26*, 126–134.
- (18) Ballantine, D. S.; White, R. M.; Martin, S. J.; Ricco, A. J.; Frye, G. C.; Zellers, E. T.; Wohltjen, H. *Acoustic Wave Sensors: Theory, Design, and Physicochemical Applications*; Academic Press: Boston, MA, 1996.
- (19) Littlewood, A. B. *Gas Chromatography*; Academic Press: New York, 1970; pp 44–121.

parameters in conjunction with linear solvation energy relationships (LSER) have been the most successful in this regard,<sup>21–25</sup> and the concepts underlying such models have been incorporated into the design and analysis of various vapor sensor array technologies employing polymers as chemically sensitive interfaces.<sup>22–27</sup> For SAW sensors, however, the combined influence of mass-loading and viscoelastic changes on many polymer-coated sensor responses<sup>28–30</sup> can reduce the accuracy of response estimates derived from LSER models, since only mass-loading effects are accounted for explicitly in the models. Applying correction factors to account for viscoelastic contributions or determining the solvation parameter coefficients for the polymers empirically from the sensor responses themselves, rather than from chromatographic retention data, can improve the accuracy of response estimations.<sup>22,23</sup>

Even where accurate estimates of SAW sensor responses are possible, a number of questions still remain about the performance of the sensor array: Are the response patterns obtained *unique enough* to differentiate all the vapors that might be encountered? What is the likelihood of errors in vapor recognition? Which vapors will be the most difficult to differentiate? What influences do random or systematic variations in sensor responses have on the analysis? To what extent do the absolute or relative vapor concentrations affect performance? While a few of these questions can be answered through conventional pattern recognition analyses of calibrated sensor responses,<sup>10</sup> or through the application of artificial neural networks (ANN)<sup>6,11</sup> or other statistical analyses,<sup>31</sup> most of them can only be answered through extensive data collection. Since this becomes intractable if more than a few vapors are being considered, the limits of performance of sensor arrays are rarely well-defined.

In a series of recent studies, we have explored the use of Monte Carlo simulation in conjunction with extended disjoint principal components regression (EDPCR) and ANN analyses for optimizing the selection of polymer coatings for SAW sensor arrays and for assessing the accuracy of recognition and quantification of individual vapors and vapor mixture components.<sup>16,32–35</sup> This

approach to sensor array design and evaluation reduces the need for exhaustive validation testing by simulating the variations expected in sensor responses in typical operation and providing precise statistical estimates of vapor-specific recognition and quantification error rates.

Another useful diagnostic application for this statistical modeling is to explore the performance of a sensor array as vapor concentrations approach the limit of detection (LOD). The LOD is one of the more important performance parameters of a chemical sensor. It is defined as the minimum detectable quantity or concentration of an analyte and is calculated from the minimum detector response, typically at some level of statistical confidence.<sup>36</sup> In the context of a vapor sensor array, or any instrument where multiple signals are required for qualitative vapor analysis, there are other considerations. If the LOD is defined strictly as the lowest detectable concentration, then it would correspond to the concentration producing the smallest signal from the most sensitive sensor. But this assumes that the identity of the analyte is known or is unimportant. If *recognition* of the analyte is required, which is arguably the main reason for using an array of sensors, the LOD must be defined as the concentration producing signals from at least two sensors (possibly all sensors) in the array to allow for analyte differentiation.

For the case where all sensors in the array are needed to unequivocally recognize a specific analyte from among a set of potential interferences, the LOD for the array as a whole would logically be defined as the concentration resulting in a detectable signal from the least sensitive sensor in the array (i.e., the sensor with the highest LOD). However, the assumption that having measurable signals from all sensors is sufficient to recognize the analyte may not be valid, since at lower concentrations the influence of electronic noise, systematic variations in sensor responses, and/or the presence of other species may preclude such a determination.

Although the difficulty in recognizing vapor response patterns at low concentrations has been discussed in previous studies,<sup>10,16</sup> the possibility of quantifying recognition error and using it to evaluate the performance of sensor arrays has not been explored. Here, we examine this issue and propose that a new parameter, which we refer to as the limit of recognition (LOR), be adopted as an additional measure of sensor array performance in the low-concentration limit.

Following brief descriptions of the data set employed and the EDPCR–Monte Carlo methodology, details are given about the various error models used for Monte Carlo simulation. Results of conventional correlation and hierarchical cluster analyses of the data are then presented for reference in subsequent discussions. Next, we use the EDPCR–Monte Carlo method to illustrate the influence of the statistical error model and vapor concentration on the nature and number of recognition errors predicted to occur. We then determine the LOR concentrations for all vapors in the data set and finally show how the LOR can be reduced by applying an additional discriminant derived from residual error analysis.

**Data Set Description.** The response data used in this study were collected as part of a previous study focused on developing an instrument for rapid measurement of organic vapors in

- (20) Abraham, M. H.; Whiting, G. S.; Doherty, R. M.; Shuely, W. J. *J. Chromatogr.* **1991**, *587*, 229–236.
- (21) Grate, J. W.; Abraham, M. H. *Sens. Actuators B* **1991**, *3*, 85.
- (22) Patrash, S. J.; Zellers, E. T. *Anal. Chem.* **1993**, *65*, 1055.
- (23) Grate, J. W.; Patrash, S. J.; Abraham, M. H. *Anal. Chem.* **1995**, *67*, 2162.
- (24) McGill, R. A.; Abraham, M. H.; Grate, J. W. *CHEMTECH* **1994**, *24*, 27.
- (25) Grate, J. W.; Patrash, S. J.; Abraham, M. H.; Dau, C. M. *Anal. Chem.* **1996**, *68*, 913–917.
- (26) Grate, J. W.; Abraham, M. H. *Proceedings of the SPIE Pacific Northwest Fiber Optic Sensor Workshop*, Troutdale, OR; SPIE: Bellingham, WA, 1995; Vol. 2574, pp 71–77.
- (27) Sugimoto, I.; Nakamura, M.; Kuwano, H. *Sens. Actuators B* **1996**, *36*, 342–347.
- (28) Grate, J. W.; Klusty, M.; McGill, R. A.; Abraham, M. H.; Whiting, G.; Andonian-Haftvan, J. *Anal. Chem.* **1992**, *64*, 610.
- (29) Martin, S. J.; Frye, G. C.; Senturia, S. D. *Anal. Chem.* **1994**, *66*, 2201.
- (30) Grate, J. W.; Kaganove, S. N.; Bhethanabotla, V. R.; *Anal. Chem.* **1998**, *70*, 199–203. Bodenhofer, K.; Hierlemann, A.; Noetzel, G.; Weimar, U.; Gopel, W. *Anal. Chem.* **1996**, *68*, 2210–2218.
- (31) Berrie, P. G. In *Handbook of Biosensors and Electronic Noses*; Kress-Rogers, E., Ed.; CRC Press: Boca Raton, FL, 1997; pp 469–500.
- (32) Zellers, E. T.; Han, M. *Anal. Chem.* **1996**, *68*, 2409–2418.
- (33) Groves, W. A. Ph.D. dissertation, University of Michigan, 1997.
- (34) Groves, W. A.; Frye, G. C.; Zellers, E. T. *Proceedings of the Symposium on Chemical and Biological Sensors and Analytical Electrochemical Methods*, Electrochemical Society Meeting, Paris, France, Aug 31–Sept 5, 1997; Ricco, A. J.; Butler, M. A.; Vanysek, P.; Horvai, G.; Silva, A. F., Eds.; Electrochemical Society: Pennington, NJ, 1997; Vol. 97–19, pp 179–190.

- (35) Groves, W. A.; Zellers, E. T. University of Michigan, 1997, unpublished work.
- (36) Hubaux, A.; Vos, G. *Anal. Chem.* **1970**, *42*, 849–855.

Table 1. Threshold Limit Value (TLV), Calibration Range, Sensitivity, and LOD for Each Test Vapor

chemical	TLV <sup>a</sup> (mg/m <sup>3</sup> )	calib range (mg/m <sup>3</sup> )	sensitivity (LOD) <sup>b</sup>			
			PIB	PDPP	PECH	OV275
benzene (BEN)	32	4–200	3.14 (4.4)	2.42 (5.4)	3.18 (23)	1.91 (25)
toluene (TOL)	188	5–1000	8.75 (1.1)	5.17 (3.7)	6.98 (2.3)	3.54 (9.0)
ethylbenzene (ETB)	434	6–1800	16.5 (0.79)	9.18 (2.4)	9.78 (5.8)	4.32 (9.0)
<i>m</i> -xylene (XYL)	434	4–1600	17.8 (0.56)	8.66 (3.5)	10.0 (2.8)	4.04 (5.2)
dichloromethane (DCL)	174	10–730	0.965 (10)	1.17 (11)	1.73 (17)	1.87 (21)
halothane (HAL)	403	30–1700	0.871 (34)	0.683 (34)	0.783 (40)	1.02 (29)
1,1,1-trichloroethane (TCA)	1900	20–1300	1.83 (5.5)	1.28 (8.6)	1.33 (7.5)	0.732 (38)
trichloroethylene (TCE)	268	9–1300	4.72 (2.1)	2.63 (3.8)	2.74 (8.8)	1.64 (24)
perchloroethylene (PCE)	170	10–630	11.2 (0.89)	4.03 (3.0)	3.32 (22)	1.48 (28)
tetrahydrofuran (THF)	590	14–2800	2.69 (12)	2.22 (9.9)	4.18 (13)	2.29 (39)
1,4-dioxane (DOX)	90	10–740	3.72 (17)	3.83 (20)	10.2 (9.2)	6.87 (18)
methoxyflurane (MOF)	169	10–1700	2.39 (6.3)	2.72 (5.5)	3.57 (7.6)	3.42 (19)
acetone (ACE)	1780	35–1900	0.842 (72)	1.25 (8.0)	3.35 (12)	3.45 (12)
2-butanone (MEK)	590	14–1500	1.94 (15)	2.43 (9.9)	5.98 (4.5)	4.78 (20)
2-propanol (IPA)	983	25–3800	0.912 (14)	0.964 (28)	2.45 (16)	3.65 (26)
1-butanol (BTL)	152	6–730	4.84 (5.0)	4.57 (11)	12.3 (3.5)	13.1 (3.9)

<sup>a</sup> Ref 41. <sup>b</sup> Sensitivity given in Hz/(mg/m<sup>3</sup>), LOD given in mg/m<sup>3</sup>; see text for definitions of acronyms for polymer sensor coatings.

breath.<sup>33–35,37–39</sup> A prototype instrument was employed that housed an array of four SAW resonators operating at 250 MHz, an adsorbent preconcentrator, and a microprocessor-controlled pneumatic system for sample capture and transport. Sensor coatings of polyisobutylene (PIB), poly(diphenoxyposphazine) (PDPP), polyepichlorohydrin (PECH), and bis-cyanoallyl polysiloxane (OV-275) were used, with each applied by airbrush in a volatile solvent to a 225-kHz frequency shift.

Each analysis entailed collection of a 0.25-L sample of exhaled breath spiked with a known concentration of an organic vapor. The vapor was retained by the preconcentrator, stripped of the majority of coadsorbed water vapor with a stream of dry air, and then thermally desorbed as an enriched, narrow pulse presented to the array for analysis in a dry-air matrix. A heating rate of 15 °C/s was used for desorption, resulting in vapor elution within 20–40 s of the start of heating. An entire sampling and analytical cycle required from 7 to 10 min. Response maxima determined from the shifts in sensor frequencies (hertz) were measured over a range of concentrations for each of the 16 vapors tested.

These data are summarized in Table 1. All response curves were linear over the calibrated concentration ranges ( $r^2 \geq 0.99$ ), and the sensitivity for each vapor-sensor pair was taken as the slope of the curve obtained from linear regression analysis with forced zero. The LOD was defined as the vapor concentration corresponding to  $3\sigma/(\text{sensitivity})$ , where  $\sigma$  is the standard deviation of the baseline response (hertz) at the time corresponding to the maximum sensor response, as determined by averaging the baseline response for at least three blank (i.e., unspiked) breath analyses. Note that the sensor providing the lowest LOD was not always the same as that providing the highest sensitivity. This is due to differences in baseline response variability, which generally was higher for OV-275 and PECH than for PIB and PDPP due to their greater sensitivity to residual water vapor in the desorbed breath samples. Some day-to-day variation in baseline stability was also observed, leading to slightly different

values of  $\sigma$  in the LOD calculations for a given sensor among the different vapors. Further details about the design and operation of the prototype instrument, the selection of preconcentrator adsorbents, and the modeling and assessment of performance are given elsewhere.<sup>33–35,37–39</sup>

**Analytical Approach and Monte Carlo Error Model Descriptions.** The modeling approach used in this study is similar to that we reported previously.<sup>16,32,35</sup> The four SAW sensor responses to each vapor challenge are summed to yield a vector in four-dimensional space, and the collection of responses over a range of concentrations is modeled using principal components. With EDPCR, each vapor is represented by an individual principal components model determined by regression of the mean-centered response vectors. Responses to binary mixtures were also collected in the original study and were modeled in this way. However, for the purposes of this initial exploration of the LOR concept, we have limited consideration to the analysis of individual vapors and their discrimination from the other 15 vapors in the calibration set.

As stated above, coupling EDPCR analysis with Monte Carlo simulations provides a means for testing the robustness of the array. Random and systematic errors are applied to the calibrated responses to all of the vapors and assumed to have a Gaussian distribution. By iteratively sampling from the resultant distributions of error-enhanced responses and treating each sample as an unknown, which is then assigned an identity using the EDPCR models established from the calibration data, the nature and statistical likelihood of recognition errors expected under typical operating conditions can be evaluated.

The success of Monte Carlo simulation depends on the accuracy with which response errors encountered in actual sensor operation are portrayed in the models used. Three error models were examined. The first includes terms representing random variation in both the sensitivity and baseline noise of each sensor (model 1), and the second model (model 2) includes the same terms as in model 1 except that the sensitivity variations are constrained to be of the same sign for all four sensors. The third model (model 3) uses the same fractional sensitivity variations

(37) Groves, W. A.; Zellers, E. T. *Am. Ind. Hyg. Assoc. J.* **1996**, *57*, 257–263.

(38) Groves, W. A.; Zellers, E. T. *Am. Ind. Hyg. Assoc. J.* **1996**, *57*, 1103–1108.

(39) Groves, W. A.; Zellers, E. T.; Frye, G. C. *Anal. Chim. Acta* **1998**, *371*, 131–143.



for all sensors, retains the random baseline variation term used in models 1 and 2, and also includes a third term to simulate response variations due to small fluctuations in residual water vapor arising from differences in the background humidity in captured samples.

The simulated response data for model 1 are generated according to the following equation:

$$r'_i = \underbrace{r_i(1 + k_1\alpha_i)}_{\substack{\text{sensitivity} \\ \text{error}}} + \underbrace{k_2\beta_i}_{\substack{\text{random} \\ \text{noise}}} \quad (1)$$

where  $r_i$  is the error-enhanced (synthetic) response for coated sensor  $i$ ,  $r_i$  is the initial ("true") response value generated by randomly selecting a point on the regression line derived from calibration,  $k_1$  is the relative standard deviation (RSD) of the sensitivity,  $k_2$  is the root-mean-square (rms) error in the sensor baseline (in hertz), and  $\alpha$  and  $\beta$  are independent, normally distributed variables with zero mean and a standard deviation of 1. This two-term error model applies different values of  $\alpha$  and  $\beta$  to each sensor for each simulated exposure.<sup>16,32</sup> It is considered the least restrictive of the three models used because it makes the fewest assumptions about sensor behavior. Values of  $k_1$  and  $k_2$  are estimated from the calibration data as described below.

Practically, it would be rare for variations in sensitivity to be truly independent. In model 2, the synthetic response for each sensor is generated using a different value of  $\alpha$ , but all  $\alpha$  values are transformed to be either positive or negative, as dictated by the sign of the  $\alpha$  value obtained for the first sensor from a given simulation. This model addresses possible variations in sensitivity arising from systematic errors in test-atmosphere generation during calibration. Such errors would vary more or less randomly around the slope of the regression line for each sensor but for a given exposure would have the same sign for all four sensors.

To generate the synthetic responses with model 3, the following equation is used:

$$r'_i = \underbrace{r_i(1 + k_1\alpha)}_{\substack{\text{proportional} \\ \text{error}}} + \underbrace{k_2\beta_i}_{\substack{\text{random} \\ \text{noise}}} + \underbrace{k_3\gamma}_{\text{RH}} \quad (2)$$

In model 3, the proportional error term replaces the sensitivity error term from models 1 and 2. The same  $\alpha$  value is applied to all four sensors for each simulated exposure because the proportional error term is meant to represent the influence of fluctuating sample volumes and/or changes in preconcentrator retention or desorption characteristics—such factors would affect all sensors to the same fractional extent and in the same direction. The random noise term in eq 2 is the same as those in models 1 and 2. The RH error term accounts for small changes in residual water vapor contained in the desorbed samples, where  $k_3$  is the RMS error in the average response attributable to this factor and  $\gamma$  is an independent normally distributed variable with zero mean and unit standard deviation. For each simulated exposure, the same value of  $\gamma$  is applied to all sensors, but different values of  $k_i$  are used for each sensor to reflect the differences in water-vapor sensitivity (see below).

A value of 0.05 was used for  $k_1$  in eqs 1 and 2 on the basis of repeated measures of the sample volume collected with the instrument—the standard deviation around the mean sample volume was about 5%. A value of 5 Hz was used for  $k_2$  because this represented a typical level of random variation in baseline frequency with clean air passing across the sensors in the array. Similar levels of baseline noise have been reported elsewhere for sensors operating at similar frequencies.<sup>40</sup> The value of  $k_i$  (eq 2) assigned to each sensor was the standard deviation of the water-vapor response peak determined from a series of unspiked breath analyses. The standard deviations were 5.4, 7.5, 12, and 15 Hz for the sensors coated with PIB, PDPP, PECH, and OV-275, respectively. These follow the order of relative water-vapor sensitivities of these coated sensors observed here and in our previous study.<sup>32</sup> The RH error term thus applies different amounts of error to each sensor but constrains the errors to be of the same sign for a given simulated exposure (via  $\gamma$ ), as would be expected for changes in relative humidity.

Temperature effects were not included in this error model for several reasons. First, the temperature of the array was actively controlled in the instrument used, and there was no evidence of temperature-induced baseline shifts during operation. In addition, our previous studies indicated that the fractional change in vapor sorption associated with small temperature shifts is small and affects most sensors similarly.<sup>32</sup> These small changes would be subsumed by the proportional error term in eq 2.

For each simulated exposure, the sum of the synthetic responses from all four sensors is treated as a vector from an "unknown" vapor and analyzed by EDPCR. The identity of this unknown is determined by the proximity of the synthetic vector to the previously stored response vectors for all vapors constructed from the calibrated sensitivities given in Table 1. This entails calculation of the Euclidean distance between the synthetic unknown vector and the vector of each of the 16 vapors. The result is a set of 16 residual error terms,  $e_1 - e_{16}$ , which are ranked in order of increasing magnitude. The unknown is then provisionally assigned the identity of the vapor giving the smallest residual error,  $e_1$ .

To verify the assignment, the vapor concentration is calculated by principal component regression. If the calculated concentration falls outside of the calibration range for the vapor, then the assignment is rejected and the vapor is assigned the identity of the vapor giving the next smallest residual error,  $e_2$ . The concentration is again calculated, and so on (note: the allowed concentration range was expanded 10% beyond the actual calibration range to account for the fact that the Monte Carlo procedure will occasionally generate a simulated exposure concentration exceeding the calibration boundaries). This process is continued until both criteria (i.e., smallest residual error and response within the allowed concentration range) are met.

This procedure of generating synthetic responses and assigning identities is performed iteratively (i.e., at least 100 simulations per vapor) to obtain a statistical estimate of the reliability of recognizing a given individual vapor from among the set of 16 possible vapors on the basis of the response pattern. Logging

(40) Grate, J.; Klusty, M. *Anal. Chem.* **1991**, *63*, 1719–1727.

(41) The American Conference of Governmental Industrial Hygienists. *1996–1997 Threshold Limit Values for Chemical Substances and Physical Agents and Biological Exposure Indices*; ACGIH: Cincinnati, OH, 1997; pp 55–69.

Table 2. Sixteen-Vapor Pairwise Correlation Matrix Derived from the Sensor Array Responses

	BEN	TOL	ETB	XYL	DCL	HAL	TCA	TCE	PCE	THF	DOX	MOF	ACE	MEK	IPA	BTL
BEN	1															
TOL	0.937	1														
ETB	0.813	0.956	1													
XYL	0.815	0.963	0.997	1												
DCL	-0.418	-0.631	-0.823	-0.790	1											
HAL	-0.505	-0.354	-0.353	-0.293	0.447	1										
TCA	0.831	0.948	0.992	0.981	-0.842	-0.466	1									
TCE	0.759	0.935	0.993	0.996	-0.822	-0.250	0.973	1								
PCE	0.636	0.863	0.960	0.965	-0.846	-0.130	0.926	0.984	1							
THF	0.707	0.448	0.172	0.190	0.333	-0.299	0.193	0.103	-0.055	1						
DOX	0.173	-0.120	-0.406	-0.377	0.816	0.074	-0.402	-0.450	-0.563	0.816	1					
MOF	-0.237	-0.508	-0.738	-0.712	0.972	0.250	-0.737	-0.763	-0.827	0.518	0.915	1				
ACE	-0.294	-0.522	-0.742	-0.706	0.991	0.414	-0.763	-0.747	-0.788	0.449	0.881	0.985	1			
MEK	-0.047	-0.327	-0.590	-0.559	0.923	0.204	-0.592	-0.620	-0.705	0.668	0.975	0.980	0.962	1		
IPA	-0.531	-0.647	-0.795	-0.749	0.952	0.699	-0.848	-0.758	-0.733	0.140	0.663	0.858	0.929	0.798	1	
BTL	-0.273	-0.465	-0.684	-0.638	0.973	0.527	-0.722	-0.674	-0.701	0.436	0.859	0.948	0.988	0.937	0.952	1

the results of each simulation permits an assessment not only of the overall rate of recognition error but also of the identities of any incorrect assignments. These results can then be presented in a so-called confusion matrix to provide added information on the performance of the array (see below).

To explore the effect of concentration and to determine the LOR for each vapor, simulations were performed within different concentration intervals, spanning a range from 1 to 50 times the LOD, where the LOD for the vapor under consideration is defined as that of the highest individual LOD among the sensors in the array. In other words, the LOD is defined as the concentration producing detectable signals in all four sensors in the array. Rates of correct recognition were then calculated as a function of concentration.

Invariably, errors in recognition increase as the vapor concentration decreases. To compare results for different vapors, a standardized error threshold must be defined that specifies the point at which the recognition error rate becomes unacceptably high. This is an arbitrary decision that depends on the consequences of making a wrong assignment of identity, among other things. For the purposes of this investigation, we have defined the LOR as the concentration below which the error rate is greater than 5%.

EDPCR modeling and Monte Carlo simulations were performed on a desktop computer using routines written in Visual Basic (Version 7.0, Microsoft Corp.) and linked to spreadsheets in Excel (Version 7.0, Microsoft Corp.). Additional statistical analyses were performed using SPSS (Version 7.0, SPSS, Inc., Chicago, IL).

## RESULTS AND DISCUSSION

**Correlation Matrix and Dendrogram.** The normalized response patterns for all vapors were constructed from the calibrated sensitivities in Table 1. Figure 1 shows a subset of these. Each panel in Figure 1 presents the relative responses of the four sensors for a particular vapor, as determined by dividing the slope of the calibration curve for each sensor by the sum of the slopes for all four sensors. Visual inspection reveals the similarity of the *m*-xylene and TCE response patterns. The benzene pattern is also similar to those of *m*-xylene and TCE, but unique features are apparent. In contrast, the pattern for

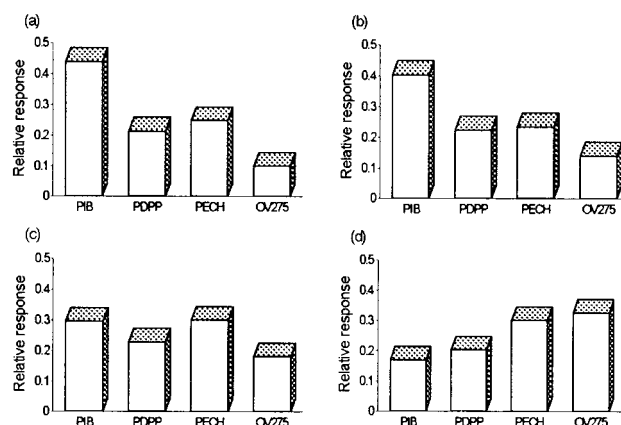


Figure 1. Normalized relative response patterns for (a) *m*-xylene, (b) trichloroethylene, (c) benzene, and (d) dichloromethane.

dichloromethane is distinctly different from the other three patterns shown.

The similarities in response patterns among all pairs of individual vapors can be evaluated quantitatively by correlation analysis. Table 2 shows the matrix of pairwise correlation coefficients ( $r$ ) for all 16 vapors. The  $r$  values corresponding to the vapors represented in Figure 1 follow the expected trend and reflect the difficulty expected in discrimination:  $r = 0.996$  for *m*-xylene with TCE;  $r = 0.815$  for benzene with xylene;  $r = 0.759$  for benzene with TCE; and  $r = -0.790$ ,  $-0.822$ , and  $-0.418$  for the pairwise correlations of dichloromethane with the other three vapors.

An alternative way of assessing the uniqueness of response patterns is illustrated in the dendrogram shown in Figure 2, which was derived from a hierarchical cluster analysis. The horizontal axis is the rescaled Euclidean distance in four-dimensional space among all of the response vectors in the data set. Those vapors linked nearer to the base (i.e., left-most axis) of the dendrogram have response vectors that are more similar to each other than those whose linkages are further from the base. The advantage of this approach to comparing response patterns is that it examines the entire data set simultaneously, rather than pairwise as in the correlation analysis. The linkages in the dendrogram are consistent with the similarities observed in the response patterns in Figure 1 and the corresponding  $r$  values in Table 2.

Table 3. Rate of Recognition as a Function of Concentration and Monte Carlo Error Model<sup>a</sup>

trial	concn range (modifications to eq 2)	recognition rate, % <sup>b</sup>		
		model 1	model 2	model 3
1	(5–50)LOD	96.7 (2.2)	96.8 (2.0)	99.9 (0.1)
2	(1–50)LOD	96.1 (2.7)	96.2 (2.6)	99.4 (0.3)
3	(1–5)LOD	94.1 (2.9)	95.6 (2.5)	92.6 (4.1)
4	(1–5)LOD (RH error = 0)			98.5 (0.9)
5	(1–5)LOD (RH error = 0, $k_2 = 10$ Hz)			91.8 (3.6)
6	(1–5)LOD (2RH error, $k_2 = 10$ Hz)			80.9 (8.3)
7	(1–5)LOD (10 vapors only)			97.5 (2.3)

<sup>a</sup> 500 iterations per vapor; see text for error model terms. <sup>b</sup> Values in parentheses define the 95% confidence interval.

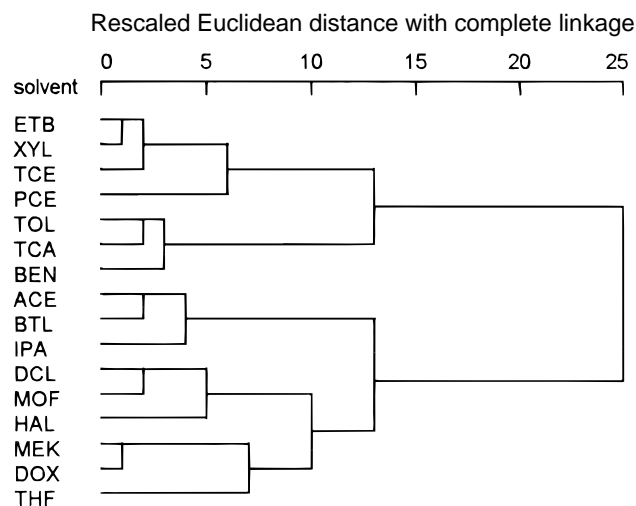


Figure 2. Dendrogram depicting linkage distances derived from hierarchical cluster analysis.

These representations of the data are typical of the extent of analysis performed to assess sensor array performance. While some insight is gained about the uniqueness of response patterns, it is not possible to determine the extent to which high  $r$  values or close linkages translate into errors in recognition and discrimination. In the context of defining an LOR, one would expect a correlation between the average  $r$  value or average linkage distance for a vapor and the concentration corresponding to the LOR, since errors in recognition would be expected at higher concentrations for vapors whose response patterns are more similar. Thus, the  $r$  values and linkage distances serve as references to which the LOR values can be compared.

**Comparison of Monte Carlo Error Models.** Before proceeding with the LOR determinations, the sensitivity of the EDPCR analysis to the error model assumed in the Monte Carlo simulations was examined. The range over which responses were tested was standardized to the LOD for each vapor. Intervals within the range of (1–50)LOD were used. Basing the modeled range on multiples of the LOD ensures a detectable concentration from each sensor for each vapor and also constrains the span to the same relative response range for all vapors. That is, the ratio of highest-to-lowest responses is the same for all vapors. While the concentration range differs for each vapor due to differences in sensitivity, decisions about vapor identities are made on the basis of responses (in hertz) rather than concentrations. It makes sense, therefore, to use the latter as the basis for defining the modeling boundaries.

Alternatively, one could base the modeling range on practical considerations related to the ultimate application of the array, such as occupational exposure assessment involving breath (or air) concentrations of vapors. In this case, the range might be standardized by the regulatory exposure limit for each vapor. While such an application-specific approach is also valid, for the purposes of this initial investigation of the LOR, the former approach was deemed more appropriate.

Results obtained with each Monte Carlo error model are presented in Table 3 as the overall rate of correct recognition (%) for all 16 vapors based on 500 iterations per vapor. For trials 1–3, the concentrations were allowed to span (1–50)LOD, (5–50)LOD, and (1–5)LOD, respectively. Regardless of the error model, the performance improved with increasing concentration, as expected. For model 1, however, the concentration dependence of the recognition rate is not significant, reflecting the predominant influence of sensitivity variations, relative to baseline noise, on sensor responses throughout each concentration range. For model 2, the recognition rate is slightly higher than with model 1 due to the sign constraint on the sensitivity variations. Here again, there is little concentration dependence observed in the recognition rate. In contrast, for model 3 the recognition rate is significantly lower for the lowest concentration range. This is consistent with expectations. The proportional error term does not influence the recognition rate because all sensors are affected to the same fractional extent for each simulated exposure, resulting in no change in the relative response pattern. Therefore, all of the recognition error is due to random noise and RH variations, which are much more influential at low vapor concentrations.

Model 3 was run again with the RH error term eliminated from eq 2 (trial 4). In this case, the recognition error in the (1–5)LOD range was only 1.5%. All of this error is attributable to random noise, indicating that RH error accounts for 98.5% – 92.6% = 5.9% of the error on average and that it is a more important determinant of performance than random noise in the low-concentration range. Comparing this latter result to that for trial 3 with model 1 shows that sensitivity variations among the sensors, if random and independent (as assumed in model 1), contribute somewhat more to recognition error than random noise over this concentration range (i.e., 4.4% vs 1.5%, respectively).

Trial 5 used model 3 with twice the initial random noise level (i.e.,  $k_2 = 10$  Hz), and trial 6 used model 3 with  $k_2 = 10$  Hz and with the  $k_i$  values (RH error term in eq 2) set at twice their initial values for all sensors. Significant reductions in recognition rates

Table 4. Confusion Matrices for Individual-Vapor Recognition Using Different Monte Carlo Error Models<sup>a</sup>

recognized as:	actual vapor identity															
	BEN	TOL	ETB	XYL	DCL	HAL	TCA	TCE	PCE	THF	DOX	MOF	ACE	MEK	IPA	BTL
Model 1: Overall Percent Correct, 94.1 ± 0.9% <sup>b</sup>																
benzene	492	9	0	0	0	0	1	0	0	0	0	0	0	0	0	0
toluene	6	456	0	3	0	0	29	3	0	0	0	0	0	0	0	0
ethylbenzene	0	0	427	87	0	0	2	10	0	0	0	0	0	0	0	0
<i>m</i> -xylene	0	0	55	404	0	0	2	9	0	0	0	0	0	0	0	0
dichloromethane	0	0	0	0	467	4	0	0	0	0	0	14	0	1	0	0
halothane	0	0	0	0	8	492	0	0	0	0	0	2	0	0	0	0
1,1,1-trichloroethane	2	18	6	1	0	0	430	20	0	0	0	0	0	0	0	0
trichloroethylene	0	17	12	5	0	0	36	458	0	0	0	0	0	0	0	0
perchloroethylene	0	0	0	0	0	0	0	0	500	0	0	0	0	0	0	0
tetrahydrofuran	0	0	0	0	0	0	0	0	0	500	0	0	0	0	0	0
1,4-dioxane	0	0	0	0	0	0	0	0	0	0	469	0	0	27	0	0
methoxyflurane	0	0	0	0	24	3	0	0	0	0	0	484	0	0	0	0
acetone	0	0	0	0	0	0	0	0	0	0	0	0	494	1	0	1
2-butanone	0	0	0	0	1	0	0	0	0	0	31	0	3	467	0	7
2-propanol	0	0	0	0	0	0	0	0	0	0	0	0	2	0	495	0
1-butanol	0	0	0	0	0	0	0	0	0	0	0	0	1	4	5	492
Model 2: Overall Percent Correct, 95.6 ± 2.5% <sup>b</sup>																
benzene	497	2	0	0	0	0	0	0	0	0	0	0	0	0	0	0
toluene	1	475	0	1	0	0	12	2	0	0	0	0	0	0	0	0
ethylbenzene	0	1	427	79	0	0	1	7	0	0	0	0	0	0	0	0
<i>m</i> -xylene	0	0	60	415	0	0	0	5	0	0	0	0	0	0	0	0
methylene chloride	0	0	0	0	479	1	0	0	0	0	0	9	0	0	0	0
halothane	0	0	0	0	3	492	0	0	0	0	0	0	0	0	0	0
1,1,1-trichloroethane	2	9	2	0	0	0	466	19	0	0	0	0	0	0	0	0
trichloroethylene	0	13	11	5	0	0	21	467	0	0	0	0	0	0	0	0
perchloroethylene	0	0	0	0	0	0	0	0	500	0	0	0	0	0	0	0
tetrahydrofuran	0	0	0	0	0	0	0	0	0	500	0	0	0	0	0	0
1,4-dioxane	0	0	0	0	0	0	0	0	0	0	483	0	0	29	0	0
methoxyflurane	0	0	0	0	17	1	0	0	0	0	0	491	0	0	0	0
acetone	0	0	0	0	0	0	0	0	0	0	0	0	496	0	0	0
2-butanone	0	0	0	0	0	0	0	0	0	0	17	0	4	470	0	4
2-propanol	0	0	0	0	0	0	0	0	0	0	0	0	0	0	495	0
1-butanol	0	0	0	0	0	0	0	0	0	0	0	0	0	1	5	496
Model 3: Overall Percent Correct, 92.6 ± 4.1% <sup>b</sup>																
benzene	480	32	0	0	0	0	26	1	0	1	0	0	0	0	0	0
toluene	14	429	2	9	0	0	9	7	0	0	0	0	0	0	0	0
ethylbenzene	0	11	398	51	0	0	21	47	0	0	0	0	0	0	0	0
<i>m</i> -xylene	0	18	50	394	0	0	15	29	1	0	0	0	0	0	0	0
methylene chloride	0	0	0	0	468	10	0	0	0	0	0	15	0	3	3	0
halothane	1	0	0	0	10	468	8	0	0	0	0	2	0	0	0	0
1,1,1-trichloroethane	1	10	3	4	0	0	408	14	0	0	0	0	0	0	0	0
trichloroethylene	0	0	47	42	0	0	12	402	0	0	0	0	0	0	0	0
perchloroethylene	0	0	0	0	0	0	0	0	499	0	0	0	1	0	0	0
tetrahydrofuran	4	0	0	0	0	0	0	0	0	498	0	2	0	0	0	0
1,4-dioxane	0	0	0	0	0	0	0	0	0	1	500	0	0	6	0	0
methoxyflurane	0	0	0	0	13	4	0	0	0	0	0	481	0	0	0	0
acetone	0	0	0	0	0	0	0	0	0	0	0	0	498	0	0	0
2-butanone	0	0	0	0	0	0	0	0	0	0	0	0	0	491	0	1
2-propanol	0	0	0	0	0	0	0	0	0	0	0	0	0	0	497	1
1-butanol	0	0	0	0	0	0	0	0	0	0	0	0	1	0	0	498

<sup>a</sup> Concentration range = (1–5)LOD;  $k_1$  = 5%,  $k_2$  = 5 Hz (see text for  $k_1$  values); 500 iterations/vapor. <sup>b</sup> 95% confidence interval.

are observed in both cases, demonstrating that controlling baseline noise and, perhaps more importantly, RH fluctuations is critical to pattern recognition in this concentration range. Of course, by doubling  $k_2$ , we have effectively doubled the LOD for the array, and much of the recognition error in trials 5 and 6 can be attributed to this factor. However, it would not be unusual to observe such increases in baseline noise in transferring from a well-controlled laboratory environment where calibrations are performed (and LODs established) to a field measurement setting where the sensor array would be susceptible to factors that might increase noise levels.

The results in Table 3 show that the critical range of concentration is  $\leq 5$ LOD. The confusion matrices presented in Table 4 provide insight into the nature of the recognition errors occurring over this concentration range for simulations run under each of the error models (trial 3, Table 3). As shown, the pattern of errors is similar, regardless of the error model employed. That is, in general, the same vapors are confused with each other with all three models, and only the rates of error differ among the different models. An exception to this is seen with toluene, which is confused for *m*-xylene and ethylbenzene to a significantly greater extent with model 3 than with the other models. For



Table 5. Confusion Matrix for 10-Vapor Subset

	BEN	XYL	DCL	TCE	PCE	THF	ACE	MEK	IPA	BTL
benzene	495	0	0	0	0	1	0	0	0	0
<i>m</i> -xylene	2	443	0	30	0	0	0	0	0	0
dichloromethane	3	3	482	0	0	0	0	3	3	0
trichloroethylene	0	53	0	469	0	0	0	0	0	0
perchloroethylene	0	0	0	1	499	0	1	0	0	0
tetrahydrofuran	0	0	0	0	0	498	0	0	0	0
acetone	0	0	0	0	0	1	498	0	0	1
2-butanone	0	0	0	0	0	0	0	497	0	0
2-propanol	0	0	0	0	0	0	0	0	496	0
1-butanol	0	0	6	0	1	0	1	0	1	499

*m*-xylene also, model 3 predicts greater confusion with TCE than do the other models. On the other hand, confusion of 1,4-dioxane with MEK is greater in models 1 and 2.

Lower recognition rates are generally associated with vapor pairs having larger  $r$  values (Table 2). A number of exceptions to this trend are seen, however. Responses for both *m*-xylene and ethylbenzene are highly correlated with that for PCE ( $r = 0.965$  and  $0.960$ , respectively), but neither is confused for PCE with any of the error models. The large  $r$  values for toluene with *m*-xylene and ethylbenzene do not translate into errors in recognition with models 1 and 2, although they do with model 3. Dichloromethane is highly correlated with halothane, methoxyflurane, acetone, 2-propanol, and butanol but confused significantly only for halothane and methoxyflurane. Other exceptions can also be seen where a high correlation coefficient does not result in significant confusion.

Lower recognition rates are also generally found for vapors with shorter cluster linkages in Figure 2. Here again, however, errors in recognizing PCE were not observed in cases where they would be expected from the linkage distances. Also, confusion among acetone, 2-propanol, and butanol was not observed with any of the models, in contrast to what would have been expected from their linkage distances. Notably, there were no cases observed where a small (or negative)  $r$  value or a large linkage distance was associated with vapors found to have a high rate of confusion. Thus, the EDPCR–Monte Carlo approach appears to be a more discriminating indicator of expected recognition errors in the critical range of concentration, but at the same time no “false negative” relationships were detected among the results of the correlation and hierarchical cluster analyses.

It was also of interest to explore the effect of the number of possible vapors on the modeling results. To this end, six of the 16 vapors were removed from consideration, and model 3 was run again with the remaining 10 vapors using the original error term values. The vapors removed were toluene, ethylbenzene, halothane, 1,1,1-trichloroethane, 1,4-dioxane, and methoxyflurane, which were among those responsible for the greatest number of recognition errors with at least one of the other 10 vapors that were retained. The recognition rate increased as expected (trial 7, Table 3) and there was little, if any, shift in the pattern of errors (Table 5). For example, with TCE the rate of confusion with *m*-xylene was virtually the same for both data sets. One might have expected some of the confusion observed between TCE and ethylbenzene to translate into increased confusion between TCE and *m*-xylene when the ethylbenzene was removed, since the response patterns for *m*-xylene and ethylbenzene are so highly

correlated. This did not occur. Similarly, confusion of *m*-xylene for TCE did not increase substantially with removal of ethylbenzene.

To summarize this error model analysis, it appears that the particular error model employed in the Monte Carlo simulations is not highly critical to revealing the types of expected recognition errors, and that the vapors confused for one another are often, though not always, those with large pairwise  $r$  values and proximal clusters. Higher error rates occur at lower concentrations, and at  $>5\text{LOD}$  the error rates become very low and nearly invariant for all vapors and all models. The level of applied error has important consequences for the recognition rate, but the nature of the recognition errors remains similar, regardless of the applied error level. Removal of certain vapors from the data set also influences expected outcomes, but translation of recognition errors among vapors with highly correlated response patterns does not seem to occur to any significant extent. The three-term error model (model 3) with the initial levels of applied error used above was adopted for further testing because it is considered to provide the most accurate portrayal of variations in sensor responses expected during actual operation.

**LOR Determinations.** To determine the LOR for each vapor, exposure simulations were repeated with model 3 within concentration intervals ranging in width from 1 to  $25\text{ mg/m}^3$ , starting at  $5\text{LOD}$  and proceeding down to  $0.5\text{LOD}$  for each of the 16 vapors. The size of the interval was determined by the magnitude of the LOD. Within each interval, from 100 to 1000 iterations were performed to get a stable statistical estimate of recognition error (larger intervals demanded a greater number of iterations). The range was extended below the LOD to explore performance trends as at least one sensor's contribution to the response pattern became statistically insignificant. Each synthetic “unknown” response vector was assigned an identity on the basis of  $e_1$ , as described above, provided that the resulting vapor was within the range of concentration defined by  $(0.45\text{--}5.5)\text{LOD}$ .

Figure 3a shows a typical set of results, in this case for toluene, where the shaded regions within an interval represent the fraction of cases where toluene was incorrectly identified as one of the other 15 vapors. As shown, the recognition rate declines to about 50% at the LOD of  $9\text{ mg/m}^3$ . The LOR (i.e., the lower limit of the concentration interval within which the correct recognition rate first declines to 95%) is at about 2.7 times the LOD concentration, or  $24\text{ mg/m}^3$  (note: if a criterion of 90% recognition is used to define the LOR, it is reduced to about  $21\text{ mg/m}^3$ , which is still  $2.3\text{LOD}$ ). While the most common error in recognition was where toluene was identified as either benzene or *m*-xylene, there were

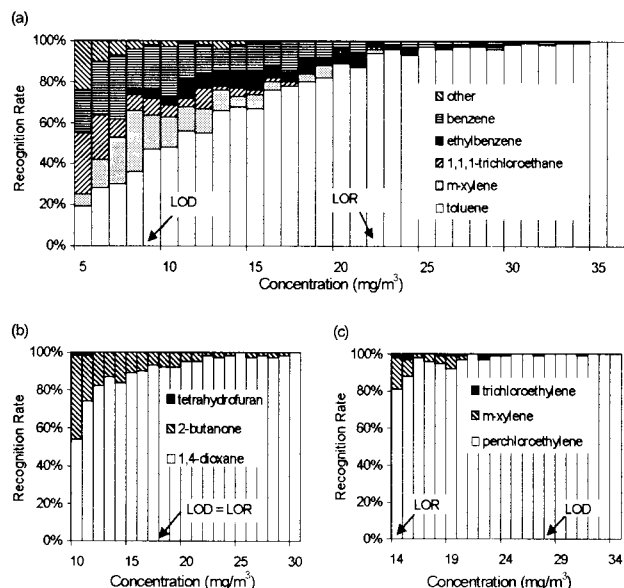


Figure 3. Plots of correct recognition versus concentration for (a) toluene, (b) 1,4-dioxane, and (c) perchloroethylene, showing relationship of LOR and LOD and the nature of the recognition errors.

several other types of recognition errors. These observations are consistent with the entries in the confusion matrix for model 3 (Table 4). Similarly, the  $r$  values (Table 2) and linkage distances (Figure 2) also reflect the most common vapor recognition errors.

Figure 3b shows results for 1,4-dioxane, where the LOR is approximately equal to the LOD. In contrast to the toluene case, 1,4-dioxane is mistaken for only one other vapor, 2-butanone, until the concentration is well below the LOD, where confusion with THF occurs in a small fraction of responses. This is also consistent with the data in Figure 2 and Tables 2 and 4. As a further test, the same analysis was repeated with the 2-butanone removed. The LOR decreased from 20 to 11 mg/m<sup>3</sup> (0.5LOD), and the errors in recognition were now distributed among several vapors, predominantly THF and butanol.

Figure 3c shows that the LOR for PCE is roughly 0.5LOD. Confusion of PCE with *m*-xylene and TCE at lower concentrations would be expected on the basis of the previous analyses, but correlation analysis would also have predicted confusion of PCE with several other vapors, which is not observed. This example, and the preceding one for 1,4-dioxane without 2-butanone included, demonstrate situations where fewer than four sensors are required for vapor recognition. Determining the minimum number of sensors required for accurate vapor recognition is also being explored with this modeling approach and will be described in a subsequent publication.

Table 6 summarizes results of similar analyses for all of the vapors. The second column in the table presents the LOR as a multiple of the LOD for each vapor. For convenience, the LOR concentration has been rounded to the nearest 0.5LOD interval. In other words, if the rate of recognition became less than 95% in the interval between 1.5LOD and 2.0LOD, then the vapor was assigned an LOR of 1.5LOD, and if that occurred in the 0.5–1LOD interval, it was assigned a value of 0.5LOD. As shown, the majority of vapors (i.e., 10/16) have LOR values greater than the LOD.

Figure 4a shows a plot of  $r^*$  vs LOR, where  $r^*$  is the average of the largest five  $r$  values from Table 2 for a given vapor.

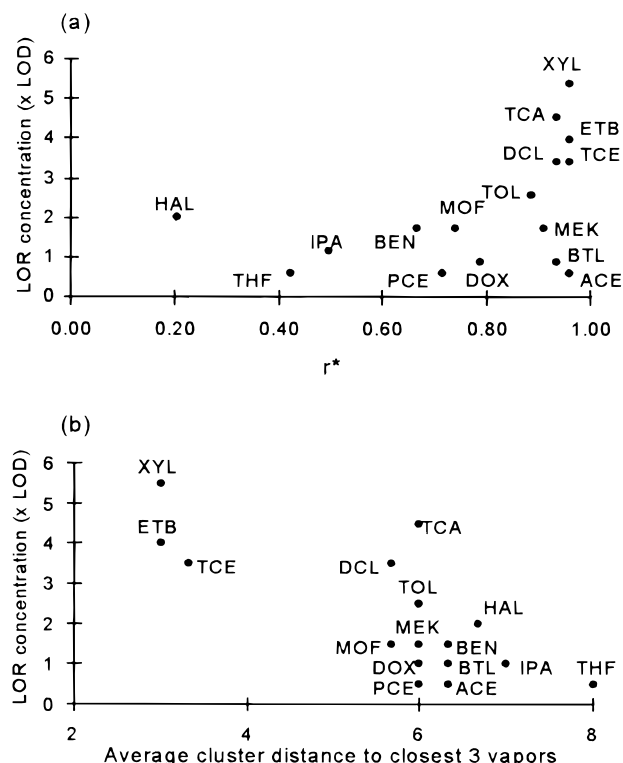


Figure 4. Plot of (a)  $r^*$  (average of five largest  $r$  values from correlation analysis) versus the LOR concentration for each vapor and (b) average linkage distance to the closest three other vapors from hierarchical cluster analysis versus the LOR concentration for each vapor.

Although the expected trend is observed, the association is weak, and correlation analysis could not be used to accurately predict the LOR concentration. Figure 4b shows a similar plot using the linkage distances derived from Figure 2 as the independent variable. The average distance from the closest three neighboring vapors gave the strongest correlation, and although it appears to be stronger than that observed using  $r^*$  as the independent variable, the linkage distance is still not a good predictor of the LOR concentration. Although this analysis was limited by the resolution of the distances provided in the hierarchical cluster analysis, it is clear that only marginal improvements would be expected, even at higher resolution.

**Reducing the LOR via Residual Error Analysis.** Since errors in recognition are related to the proximity of the synthetic response vector of the unknown vapor to alternative calibrated vapor response vectors, as well as the proximity of alternative response vectors to the correct vector, the rate of error in recognition should be related to the relative values of the residual errors  $e_1$  and  $e_2$ . These errors correspond to the Euclidean distance between the unknown vector and the closest and next-closest calibrated response vectors, respectively.

Figure 5 shows a plot of the quantity  $\Delta e$  versus concentration for TCE, where  $\Delta e = e_2 - e_1$ . The open symbols designate correctly recognized cases, and the filled symbols represent recognition errors. As shown, there is a very clear relationship between concentration and  $\Delta e$ . This trend was observed consistently for all vapors, suggesting that a threshold value of  $\Delta e$  might be used as an additional criterion for establishing the LOR (note: no correlation with concentration was observed for either  $e_1$  or  $e_2$ ).

Table 6. Limit of Recognition (LOR) for Each Vapor as a Multiple of the LOD with and without Applied Residual Error Threshold Criterion,  $\Delta e^a$

chemical	LOR	$\Delta e$	LOR <sub>e</sub>	ratio LOR/LOR <sub>e</sub>	LOR <sub>eg</sub>	ratio LOR/LOR <sub>eg</sub>
benzene	2.0 (50.0)	8.0	0.5 (12.5)	4.0	0.5 (12.5)	4.0
toluene	2.5 (22.5)	11.3	2.0 (18.0)	1.3	2.0 (18.0)	1.3
ethylbenzene	4.0 (36.0)	13.0	2.0 (18.0)	2.0	2.0 (18.0)	2.0
<i>m</i> -xylene	5.0 (26.0)	11.2	2.5 (13.0)	2.0	2.5 (13.0)	2.0
dichloromethane	3.0 (63.0)	6.3	1.5 (31.5)	2.0	0.5 (10.5)	6.0
halothane	2.0 (80.0)	6.0	0.5 (20.0)	4.0	0.5 (20.0)	4.0
1,1,1-trichloroethane	3.5 (133.0)	10.0	2.0 (76.0)	1.8	2.0 (76.0)	1.8
trichloroethylene	4.0 (96.0)	9.4	1.5 (36.0)	2.7	1.5 (36.0)	2.7
perchloroethylene	0.5 (14.0)	6.0	0.5 (14.0)	1.0	0.5 (14.0)	1.0
tetrahydrofuran	0.5 (19.5)	6.0	0.5 (19.5)	1.0	0.5 (19.5)	1.0
1,4-dioxane	1.0 (20.0)	6.0	0.5 (10.0)	2.0	0.5 (10.0)	2.0
methoxyflurane	1.5 (28.5)	7.0	1.0 (19.0)	1.5	1.0 (19.0)	1.5
acetone	0.5 (36.0)	6.0	0.5 (36.0)	1.0	0.5 (36.0)	1.0
2-butanone	1.5 (30.0)	6.0	1.0 (20.0)	1.5	0.5 (10.0)	3.0
2-propanol	0.5 (14.0)	6.0	0.5 (14.0)	1.0	0.5 (14.0)	1.0
1-butanol	1.0 (11.0)	6.0	0.5 (5.5)	2.0	0.5 (5.5)	2.0

<sup>a</sup> LOR<sub>e</sub> and LOR<sub>eg</sub> are revised LOR values determined by application of individual and global  $\Delta e$  criteria, respectively. All LOR values have been rounded down to the nearest 0.5LOD. <sup>b</sup> Values in parentheses are in units of mg/m<sup>3</sup>.

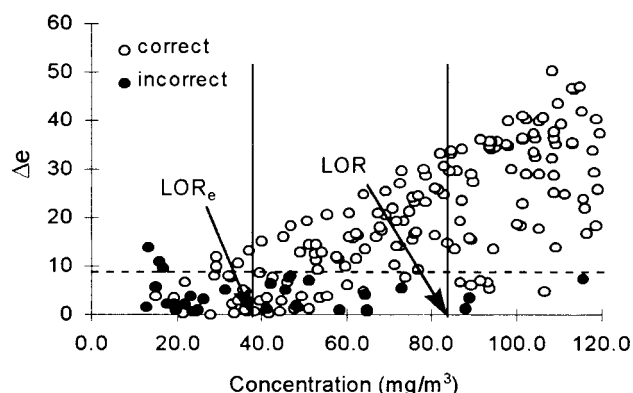


Figure 5. Plot of concentration versus  $\Delta e$  for TCE showing limit of recognition with (LOR<sub>e</sub>) and without (LOR) application of  $\Delta e$  threshold determined from residual error analysis.

alone). Since  $\Delta e$  for any synthetic response vector varies statistically, it was necessary to characterize the distribution of  $\Delta e$  in order to determine a logical threshold for each vapor. To this end, several thousand iterations of the EDPCR–Monte Carlo routine were run for each vapor to obtain at least 100 cases where an error in recognition occurred. The  $\Delta e$  distribution for the errant cases was approximately normal (though generally slightly skewed to the right as expected for a left-censored distribution), and the 95th percentile, calculated under the normality assumption, was used as the threshold  $\Delta e$  value for each vapor.

The horizontal broken line in Figure 5 shows the  $\Delta e$  threshold value for TCE. Applying this threshold as an additional criterion for recognition leads to a reduction in the LOR concentration, since a large number of correctly recognized simulated exposures falling below the original LOR concentration had  $\Delta e$  values above this threshold. For TCE, this reduces the LOR from 84 to 38 mg/m<sup>3</sup>. This revised LOR value is designated LOR<sub>e</sub> to reflect the use of the residual error threshold in its determination. As shown in Table 6, LOR<sub>e</sub> ≤ LOR for all of the vapors.

While imposing the  $\Delta e$  threshold criterion provides a means of reducing the recognition limit, to have general utility, a global value of  $\Delta e$  applicable to all vapors is needed. As shown in Table 6,  $\Delta e$  ranges from 6 to 13. The fact that the largest value is

associated with ethylbenzene means that it is the vapor most likely to be confused with one or more other vapors. The limiting value of  $\Delta e$  for the set of 16 vapors as a whole is, therefore, 13. Substituting  $\Delta e = 13$  as a threshold and repeating the analyses for all vapors gave the global recognition limits designated LOR<sub>eg</sub> in Table 6. In most cases, there is a negligible difference between LOR<sub>e</sub> and LOR<sub>eg</sub>. This is because there are very few vapors for which there was any increase in the rate (or number) of correct recognition below the LOR<sub>e</sub> concentration, regardless of the  $\Delta e$  threshold. For dichloromethane and 2-butanone, however, this is not the case, and raising the  $\Delta e$  threshold did capture an additional set of simulations giving proportionally more correct recognition. For these latter two vapors, the LOR<sub>eg</sub> values are significantly lower than the corresponding LOR<sub>e</sub> values. This demonstrates that global reductions in LOR values are possible within a given data set using a single residual error criterion.

## CONCLUSIONS

This study has illustrated the use of EDPCR pattern recognition analysis in conjunction with Monte Carlo simulations of calibrated response data for characterizing errors in vapor recognition for a polymer-coated SAW vapor sensor array in the lower concentration limit. Three different models of applied error were examined in the Monte Carlo simulations, and the number and nature of vapor recognition errors were quantified in each case. While the type of error model was found to affect the overall rate of correct recognition, similar vapors were confused for each other with all models. We favor the three-term error model (model 3) because it provides the most realistic representation of expected variations in sensor responses. But, as shown, alternative error models yield qualitatively similar results.

Analyses described herein considered the problem of recognizing response patterns of individual vapors from among a training set of 16 vapors representing several different chemical classes. Results revealed that, for most vapors, errors in recognition became significant (i.e., >5%) at concentrations well above their respective LODs. Thus, the concentration corresponding to the limit of recognition (LOR) may be more important than the

concentration corresponding to the LOD for evaluating performance at low concentrations. Although only polymer-coated SAW sensor arrays were considered here, this approach to performance modeling is applicable to other sensor technologies as well.

Unlike the LOD, the LOR for a vapor is a function of the number and types of other possible vapors present during an analysis. Therefore, the LOR must be determined on a case-by-case basis. For this data set, which included subsets of vapors that were very similar structurally, the highest LOR was approximately 5LOD. To the extent that the similarity in response patterns in this data set is typical, a general guideline might be to restrict analyses to concentrations greater than this value to avoid concentration related errors in recognition. It was shown, however, that the LOR could be reduced by the application of an additional threshold criterion derived from residual error analysis and that a global threshold value could be applied to all vapors within the data set. Testing responses against this residual error threshold could be easily incorporated into the data analysis. It should be kept in mind that analyses of vapors mixtures were not considered and may result in more restrictive (i.e., higher) LORs in certain cases. The problem of mixtures represents an additional challenge in the context of this modeling, since one must consider the similarity in response patterns of multiple vapors as well as their relative concentrations.<sup>10</sup>

Although the LOR was greater than the LOD for most of the vapors examined, for several vapors the LOR was well below the LOD. This indicates that fewer than four sensors are required in order to recognize such vapors. Determining the minimum number of sensors that is required for vapor analysis is another problem that can be addressed with this modeling approach. Tailoring the number and types of sensors to each possible exposure scenario encountered would increase the computational efficiency of the pattern recognition and would eliminate sensors providing redundant responses.

Comparisons between the results of the EDPCR–Monte Carlo modeling and those from correlation analysis and hierarchical cluster analysis showed good correspondence in most cases. That is, vapors giving high pairwise correlation coefficients or close cluster linkages were generally found to be confused for one another at low concentrations, according to the simulations. However, there were several cases where vapors that were highly correlated or closely linked were not confused for one another to any appreciable extent. Correlation coefficients and cluster distances were also found to be poor predictors of the LOR concentration.

A practical means for using recognition in a quantitative manner to establish performance boundaries for a sensor array at low concentration has been presented here. Results demonstrate the utility of Monte Carlo simulation in providing information that is inaccessible by standard pattern recognition analyses alone and that could otherwise be obtained only by exhaustive validation testing.

#### ACKNOWLEDGMENT

The authors acknowledge Dr. Gregory C. Frye-Mason of Sandia National Laboratories for valuable discussions. They also acknowledge Dr. Tin-Su Pan for writing the first version of the EDPCR routine and Mr. Mingwei Han for initial revisions to that routine. Support for this work was provided by Grant R01-OH03332 from the National Institute for Occupational Safety and Health of the Centers for Disease Control and by a contract from Sandia National Laboratories, Albuquerque, NM.

Received for review March 26, 1998. Accepted July 13, 1998.

AC980344W